ORIGINAL RESEARCH ARTICLE

CrossMark

Effects of Phenothiazines on Aldehyde Oxidase Activity Towards Aldehydes and N-Heterocycles: an In Vitro and In Silico Study

Farnaz Deris-Abdolahpour[1] · Lida Abdolalipouran-Sadegh[1] · Siavoush Dastmalchi[2,3] ·
Maryam Hamzeh-Mivehroud[2,3] · Omid Zarei[4,5] · Gholamreza Dehgan[1] · Mohammad-Reza Rashidi[3,6]

Abstract

Background Aldehyde oxidase (AOX) is an important molybdenum-containing enzyme with high similarity with xanthine oxidase (XO). AOX involved in the metabolism of a large array of aldehydes and N-heterocyclic compounds and its activity is highly substrate-dependent.

Objectives The aim of this work was to study the effect of five important phenothiazine drugs on AOX activity using benzaldehyde and phenanthridine as aldehyde and N-heterocyclic substrates, respectively.

Methods The effect of trifluperazine, chlorpromazine, perphenazine, thioridazine and promethazine on rat liver AOX was measured spectrophotometrically. To predict the mode of interactions between the studied compounds and AOX, a combination of homology modeling and a molecular docking study was performed.

Results All phenothiazines could inhibit AOX activity measured either by phenanthridine or benzaldehyde with almost no effect on XO activity. In the case of benzaldehyde oxidation, the lowest and highest half-maximal inhibitory concentration (IC_{50}) values were obtained for promethazine ($IC_{50} = 0.9$ μM), and trifluoperazine ($IC_{50} = 3.9$ μM), respectively; whereas perphenazine ($IC_{50} = 4.3$ μM), and trifluoperazine ($IC_{50} = 49.6$ μM) showed the strongest and weakest inhibitory activity against AOX-catalyzed phenanthridine oxidation, respectively. The in silico findings revealed that the binding site of thioridazine is near the dimer interference, and that hydrophobic interactions are of great importance in all the tested phenothiazines.

Conclusion The five studied phenothiazine drugs showed dual inhibitory effects on AOX activity towards aldehydes and N-heterocycles as two major classes of enzyme substrates. Most of the interactions between the phenothiazine-related drugs and AOX in the binding pocket showed a hydrophobic nature.

Key Points

All phenothiazine drugs used in this study showed inhibitory effects on AOX activity with almost no effect on XO activity.

With all tested phenothiazines, more inhibition was observed with the benzaldehyde compared with phenanthridine.

Most of the interactions between the phenothiazine related drugs and AOX in the binding pocket showed hydrophobic nature.

✉ Mohammad-Reza Rashidi
  rashidi@tbzmed.ac.ir

[1] Department of Zoology, Faculty of Natural Science, University of Tabriz, Tabriz, Iran

[2] Biotechnology Research Center, Tabriz University of Medical Sciences, Tabriz, Iran

[3] School of Pharmacy, Tabriz University of Medical Sciences, Tabriz, Iran

[4] Neurosciences Research Center, Kurdistan University of Medical Sciences, Sanandaj, Iran

[5] Cellular and Molecular Research Center, Research Institute for Health Development, Kurdistan University of Medical Sciences, Sanandaj, Iran

[6] Research Center for Pharmaceutical Nanotechnology, Tabriz University of Medical Sciences, Tabriz 51664-14766, Iran

△ Adis

1 Introduction

Although cytochrome P450 enzymes (CYP) are by far the dominant drug metabolizing systems, a shift in medicinal chemistry strategies and advancements in the field of non-CYP-mediated metabolism have caused an increase in the involvement of non-CYP-mediated metabolic pathways, and the number of compounds that serve as substrates for these enzymatic systems has rapidly increased in recent years [1–4].

Aldehyde oxidase (AOX; EC 1.2.3.1) is one of these non-CYP enzymes that can metabolize a broad range of aldehydes and N-heterocyclic compounds including some important drugs such as famciclovir [5], ziprasidone [6], 6-mercaptopurine [7], zebularine [8], and methotrexate [9]. Accordingly, the number of potential drug molecules metabolized by this enzyme has markedly increased in recent years, putting AOX a the center of attention of drug screening and discovery programs [10–12].

AOX is a cytosolic molybdenum-containing hydroxylase composed of two identical subunits of about 150 kDa, with each subunit consisting of three distinct domains. It is widely distributed through the animal kingdom, and can be found in species as diverse as the sea anemone and man. This enzyme is very closely related to an other molybdenum hydroxylase, xanthine oxidase (XO; EC 1.2.3.2), sharing very similar characteristics, such as molecular weight, cofactor composition, subunit structure, and substrate specificities (both oxidize aromatic aldehydes and N-heterocycles on an electrophilic carbon atom adjacent to an oxygen or nitrogen atoms).

Given the role of AOX in drug metabolism, it is likely that those compounds that can inhibit AOX activity interfere with the metabolism of drugs catalyzed by AOX following their co-administration. Drug interactions are of great concern as they may lead to an increase in side effects and reduce the drug efficiency [13, 14], and are considered as one of the most important leading causes of morbidity and mortality [15]. Inhibition of drug-metabolizing enzymes is a frequent cause of clinically significant drug interactions [16]. Therefore, identification of enzyme inhibitors, elucidating the mechanism of inhibition and understanding the modes of inhibitor binding are important information required for drug discovery programs, the optimization of enzyme inhibitors, and also for appropriate rational designs and the implementation of clinical studies. There are numerous reports indicating that many compounds, including some natural compounds [17, 18] and important drugs [19, 20], can act as AOX inhibitors.

Some phenothiazines such as chlorpromazine are also potent inhibitors of AOX activity [20, 21]. Phenothiazines are an important group of drugs that have been widely used to treat psychiatric disorders such as schizophrenia for over 50 years. In addition, they have a broad array of other activities such as antitumor effects, antimicrobial activity and anti-emetic action. Taking into account the extensive use of phenothiazines on the one hand, and the broad range of drugs and natural compounds that act as AOX substrates and inhibitors on the other hand, there would be great potential for drug interactions in concomitant administration of these compounds.

The inhibitory profile can be dependent on the type of the substrate used in the enzymatic reaction. This, in turn, can markedly influence in vitro drug–drug interaction prediction. Therefore, the use of a multiple substrate screening approach has been suggested as an appropriate strategy in the design of a drug–drug interaction study [22]. AOX shows extreme substrate-dependent inter- and intra-species variation, and some part of this variation arises from the type of the substrate used in the enzyme activity measurement [12]. Unlike XO activity, which is routinely monitored by xanthine as the substrate, various substrates have been used for AOX activity assays, and the selection of an appropriate substrate for AOX-based drug–drug interaction studies will be a critical issue [12]. As has been mentioned, AOX is able to oxidize a wide range of compounds which can be grouped into the two major classes of N-heterocycles and aldehydes. We have shown that the inhibitory effect of flavonoids on AOX activity measured by aldehydes as the substrate is different from assays by N-heterocyclic substrates [23]. In the present study, the inhibitory effect of phenothiazines on AOX activity has been investigated using both benzaldehyde (an aldehyde) and phenanthridine (an N-heterocycle) as the enzyme substrates. To the best of our knowledge, this is the first comparative AOX inhibition profile study using aldehyde and N-heterocyclic compounds as the enzyme substrates. This study can provide a better understanding of the function and mechanism of the AOX action.

2 Materials and Methods

2.1 Chemicals

Benzaldehyde, phenanthridine and xanthine were purchased from Sigma-Aldrich (Poole, Dorset, UK). Trifluperazine, chlorpromazine, perphenazine, thioridazine and promethazine were a kind gift from Prof. Hadi Valizadeh, Tabriz University of Medical Sciences, Tabriz, Iran. Other chemicals were purchased from Merck (Darmstadt, Germany) and were of analytical grade.

2.2 Preparation of Partially Purified AOX and XO

Six 7- to 8-week-old male Wistar rats with body weights between 250 and 300 g were obtained from the Animal House of Tabriz University of Medical Sciences, Iran, and used for the experimental studies. They were fed with a standard laboratory diet and allowed food and water ad libitum. The animals were maintained in a controlled temperature (18 ± 1 °C), humidity (50%) and lighting cycle of 07:00–19:00 hours light and 19:00–07:00 hours dark. They were handled with human care in accordance with the National Institute of Health guidelines, and the study was approved by the local and national ethic committees.

The animals were killed by general anesthesia with ether between 09:00 and 10:00 hours and the livers were quickly excised after removing the excess fat and gall bladder, and placed on ice-cold isotonic potassium chloride solution (1.15% KCl w/v) containing 0.1 mM EDTA. The livers were then homogenized on ice in a homogenizer fitted with a Teflon pestle. A partially purified molybdenum hydroxylase fraction containing both AOX and XO was prepared from the liver homogenate by heat treatment and ammonium sulphate precipitation, as described elsewhere [24]. The partially purified enzyme fractions were kept in liquid nitrogen until required.

2.3 Enzyme Assays

All the enzyme assays were carried out using a Shimadzu 2550 UV/VIS spectrophotometer. It was controlled by the Shimadzu UV Probe personal software package. The instrument was connected to a Shimadzu cell temperature-controlling unit. AOX activity was measured using phenanthridine and benzaldehyde as the substrates at 322 and 246 nm, respectively. XO activity was determined by monitoring uric acid production from xanthine at 295 nm.

The substrates were incubated separately with the enzyme fraction in Sorenson's phosphate buffer (67 mM, pH = 7.0) containing 0.1 mM of EDTA at 37 °C at a final concentration of 40 μM for phenanthridine, 100 μM for benzaldehyde and 40 μM for xanthine. The reactions were started by the addition of the enzyme fraction to the reaction solution and measured for up to 5 min for phenanthridine and benzaldehyde and 30 min for xanthine. The reactions were also carried out in the presence of phenothiazine solutions (2–50 μM), and the results were compared with the inhibitory effects of 1–100 μM menadione (an AOX-specific inhibitor) and 1–100 μM allopurinol (a potent inhibitor of XO).

2.4 Determination of Kinetic Constants

To obtain the Michaelis–Menten constant (K_m) and the maximum initial velocity (V_{max}), the AOX-catalyzed oxidation of benzaldehyde in Sorenson's phosphate buffer (67 mM, pH = 7.0 containing 0.1 mM EDTA) in the absence and presence of phenothiazines was determined. Different concentrations of benzaldehyde (10–100 μM) were incubated with the enzyme fraction at 37 °C in the absence or presence of each phenothiazine, and the initial oxidation rates were measured. K_m and V_{max} values were determined from Lineweaver–Burk double reciprocal plots of 1/[S] against 1/v. The line of the best fit through the points on the plot was calculated using linear regression by the least squares method (SPSS, v.16).

The IC_{50} values of the inhibitors were obtained from the plot of the log of more than five concentrations of the tested inhibitors versus the percent inhibition of the enzyme activities. The inhibition constants were determined using secondary plots (slopes and intercepts from the initial Lineweaver–Burk plot vs. inhibitor concentrations). In the case of mixed inhibition, where the inhibitor can bind to the free enzyme and to the enzyme–substrate complex, two inhibitor constants were defined: K_i as the dissociation constant of the enzyme–inhibitor complex, and K_I as the dissociation constant of the enzyme–substrate–inhibitor complex. If $K_i < K_I$, the inhibition was considered as a competitive–noncompetitive type; if $K_i > K_I$, the inhibition was considered as uncompetitive–noncompetitive.

2.5 Protein Determination

Protein concentrations of the partially purified enzyme fractions were determined spectrophotometrically using Bradford assay with bovine serum albumin as a standard protein.

2.6 Molecular Modeling Studies

2.6.1 Homology Modeling

The three-dimensional (3D) structure of rat AOX1 was generated by homology modeling, as outlined below. First, the amino acid sequence of rat AOX1 (Accession number: Q9Z0U5) was obtained from the UniProt database and subjected to BLAST search against the Protein Data Bank to find homologous proteins with known 3D crystal structures [25, 26]. The PDB crystal structure of human AOX1 (PDB ID: 4UHX) was selected as an appropriate template [27]. Alignment of rat and human AOX1 (UniProtKB-Q06278) sequences was performed using the ClustalOmega webserver [28]. The initial model was generated by threading the sequence of rat AOX1 onto the structure of human AOX1 guided by the sequence alignment (Fig. 1). This initial model was submitted to

```
RAT AO      -MDPPQLLFYVNGQKVVENNVDPEMMLLPYLRKNLRLTGTKYGCGGGGCGACTVMISRYNPSTKSIRHHPVNACLTPICSLYGTAVTTVEGIGNTRTRLHPVQERIAKCHSTQCGFCTPG
HUMAN AO    MDRASELLFYVNGRKVIEKNVDPETMLLPYLRKKLRLTGTKYGCGGGGCGACTVMISRYNPITKRIRHHPANACLIPICSLYGAAVTTVEGIGSTHTRIHPVQERIAKCHGTQCGFCTPG
            :*******:**:*:***** ********:*****************************:** ** *****.**** *******:*********.*.:**:**********.*********

RAT AO      MVMSMYALLRNHPEPSLDQLTDALGGNLCRCTGYRPIIDACKTFCRASGCCESKENGVCCLDQGINGSAEFQEGDETSPELFSEKEFQPLDPTQELIFFPPELMRIAEKQPPKTRVFYSNR
HUMAN AO    MVMSIYTLLRNHPEPTLDQLTDALGGNLCRCTGYRPIIDACKTFCKTSGCCQSKENGVCCLDQGINGLPEFEEGSKTSPKLFAEEEFLPLDPTQELIFFPPELMIMAEKQSQRTRVFGSER
            ****.*:*********:*************************:.****:******** :.**** :.** ** **:*.:*** ::** ***************** :**** .:**** *:*

RAT AO      MTWISPVTLEELVEAKFKYPGAPIVMGYTSVGPEVKFKGVFHPIIISPDRIEELSIINQTGDGLTLGAGLSLDQVKDILTDVVQKLPEETTQTYRALLKHLRTLAGSQIRNMASLGGHIV
HUMAN AO    MMWFSPVTLKELLEFKFKYPQAPVIMGNTSVGPEVKFKGVFHPVIISPDRIEELSVVNHAYNGLTLGAGLSLAQVKDILADVVQKLPEEKTQMYHALLKHLGTLAGSQIRNMASLGGHII
            * *:*****:**:* ***** **:.** *************:***********::*:: :********** ****** *****.** *:****** *****************:

RAT AO      SRHLDSDLNPLLAVGNCTLNLLSKDGKRQIPLSEQFLRKCPDSDLKPQEVLVSVNIPCSRKWEFVSAFRQAQRQQNALAIVNSGMRVLFREGGGVIKELSILYGGVGPTTIGAKNSCQKL
HUMAN AO    SRHPDSDLNPILAVGNCTLNLLSKEGKRQIPLNEQFLSKCPNADLKPQEILVSVNIPYSRKWEFVSAFRQAQRQENALAIVNSGMRVFFGEGDGIIRELCISYGGVGPATICAKNSCQKL
            *** ****** :************:*******.****.***:.:***** :****** ******************:************** **.:*:**.* ******.** ********

RAT AO      IGRPWNEEMLDTACRLVLDEVTLAGSAPGGKVEFKRTLIISFLFKFYLEVLQGLKREDPGHYPSLTNNYESALEDLHSKHHWRTLTHQNVDSMQLPQDPIGRPIMHLSGIKHATGEAIYC
HUMAN AO    IGRHWNEQMLDIACRLILNEVSLLGSAPGGKVEFKRTLIISFLFKFYLEVSQILKKMDPVHYPSLADKYESALEDLHSKHHCSTLKYQNIGPKQHPEDPIGHPIMHLSGVKHATGEAIYC
            *** ***.*** **** *:**:*** :**************************** *: :** *****::.*************** .:**:. * *.****:*******.***********

RAT AO      DDMPAVDRELFLTFVTSSRAHAKIVSIDLSEALSLPGVVDIITADHLQDATTFG----TETLLATDKVHCVGQLVCAVIADSETRAKQAAKHVKVVYRDLEPLILTIEEAIQHKSFFESE
HUMAN AO    DDMPLVDQELFLTFVTSSRAHAKIVSIDLSEALSMPGVVDIMTAEHLSDVNSFCFFTEAEKFLATDKVFCVGQLVCAVLADSEVQAKRAAKRVKIVYQDLEPLILTIEESIQHNSSFKPE
            ****.**:***********************:.*:******:**:**.*..:*       :*.:****** .*********.****.:**:***:**.**.:.******:***.* *: *

RAT AO      RKLECGNVDEAFKIADQILEGEIHIGGQEHFYMETQSMLVVPKGEDGEIDIYVSTQFPKHIQDIVAATLKLSVNKVMCHVRRVGGAFGGKVGKTSIMAAITAFAASKHGRAVRCTLERGE
HUMAN AO    RKLEYGNVDEAFKVVDQILEGEIHMGGQEHFYMETQSMLVVPKGEDQEMDVYVSTQFPKYIQDIVASTLKLPANKVMCHVRRVGGAFGGKVLKTGIIAAVTAFAANKHGRAVRCVLERGE
            **** ********:.**:***.******.::*******************:**:*******:********.******.:.***.******.:.:.:.****:***.:**::******.*****

RAT AO      DMLITGGRHPYLGKYKVGFMRDGRIVALDVEHYCNGGSSLDESLWVIEMGLLKMDNAYKFPNLRCRGWACRTNLPSHTALRGFGFPQAGLVTEACVTEVAIRCGLSPEQVRTINMYKQID
HUMAN AO    DMLITGGRHPYLGKYKAGFMNDGRILALDMEHYSNAGASLDESLFVIEMGLLKMDNAYKFPNLRCRGWACRTNLPSNTAFRGFGFPQAALITESCITEVAAKCGLSPEKVRIINMYKEID
            ****************.***:****:****:***.*.*.******:***************************.**:***********.*::*:*:****:*****:**::*****:**

RAT AO      NTHYKQEFSAKTLFECWRECMAKCSYSERKTAVGKFNAENSWKKRGMAVIPLKFPVGVGSVAMGQAAALVHIYLDGSALVSHGGIEMGQGVHTKMIQVVSRELKMPMSSVHLRGTSTETV
HUMAN AO    QTPYKQEINAKNLIQCWRECMAMSSYSLRKVAVEKFNAENYWKKKGLAMVPLKFPVGLGSRAAGQAAALVHIYLDGSVLVTHGGIEMGQGVHTKMIQVVSRELRMPMSNVHLRGTSTETV
            :* ****:.**.*.::*******.:*** **.** ****** ***:*:*:*:*******.:** .* **************.**:*****************.****.***********

RAT AO      PNTNASGGSVVADLNGLAVKDACQTLLKRLEPIISKNPQGTWKDWAQTAFDQSVSLSAVGYFRGYESNINWEKGEGHPFEYFVYGAACSEVEIDCLTGDHKNIRTDIVMDVGHSINPALD
HUMAN AO    PNANISGGSVVADLNGLAVKDACQTLLKRLEPIISKNPKGTWKDWAQTAFDESINLSAVGYFRGYESDMNWEKGEGQPFEYFVYGAACSEVEIDCLTGDHKNIRTDIVMDVGCSINPAID
            **:.* *********************************:***********:*:.*************:.*******.**************************************.* *****.:*

RAT AO      IGQVEGAFIQGMGLYTIEELSYSPQGILYSRGPNQYKIPAICDIPTEMHISFLPPSEHSNTLYSSKGLGESGVFLGCSVFFAIHDAVRAARQERGISGPWKLTSPLTPEKIRMACEDKFT
HUMAN AO    IGQIEGAFIQGMGLYTIEELNYSPQGILHTRGPDQYKIPAICDMPTELHIALLPPSQNSNTLYSSKGLGESGVFLGCSVFFAIHDAVSAARQERGLHGPLTLNSPLTPEKIRMACEDKFT
            ***:****************.*******:.***:*********:***:*:*.:****::****************************:*****.****.*** .** .*.*****************

RAT AO      KMIPRDEPGSYVPWNIPV
HUMAN AO    KMIPRDEPGSYVPWNVPI
            ***************:*:
```

Fig. 1 Sequence alignment used for building the homology model of rat AOX (target sequence) based on the structure of the human AOX3 crystal structure (PDB code: 4UHX the template structure). The symbols *, : and . represent identical, conserved and semi-conserved substitutions, respectively

the Swiss-Model web server for energy minimization and further geometry refinement using the GROMOSE96 force field [29]. The model quality was assessed from the geometry point of view using the MolProbity server [30] and evaluation of the atomic non-local interaction profile by ANOLEA server [31].

2.6.2 Preparation of the Ligand Structures

The 3D structures of the studied phenothiazines (i.e., chlorpromazine, perphenazine, promethazine, and trifluoperazine) were generated using HyperChem v.8 [32] and subjected to energy minimization using MM + force field [33]. Then, the structures were fully optimized based on the semi-empirical method, using the AM1 level of theory [34]. The structures were saved in HIN format, and then converted to Mol2 file format using Open Babel software [35].

2.6.3 Molecular Docking

In order to determine the binding modes between phenothiazines and rat AOX1, the studied compounds were subjected to docking calculations on the rat AOX1 model structure using GOLD v.5.0. The 3D structure of human AOX1 co-crystallized with thioridazine (4UHX) was used as the guide for determining the binding sites for the rest of the studied phenothiazines [27]. The multiple poses resulting for each of the ligands were assessed by Shape-it v.1.0.1 [36] to select the closest conformation to that of the co-crystalized thioridazine bound to the human AOX1. The results were analyzed by the LigPlot program v.1.4.5 [37].

Table 1 Chemical structures and the effects of some phenothiazines at 10 μM on the oxidation of phenanthridine and benzaldehyde catalyzed by rat liver aldehyde oxidase (AOX) and xanthine oxidation catalyzed by rat liver xanthine oxidase (XO)

Structure	Name	Inhibition percent		
		Phenanthridine	Benzaldehyde	Xanthine
	Menadione (10 μM)	91±3	78±2	31↑*
	Allopurinol (100 μM)	0.0	2±4	98±3
	Chlorpromazine	53±4	91±0	4±2↑
	Perphenazine	78±1	95±2	3±1↑
	Promethazine	56±4	96±5	4±1.41
	Thioridazine	50±0	85±1	3±3↑
	Trifluoperazine	21±6	66±4	3±2↑

*Oxidation rate increased

3 Results

3.1 Inhibition of Rat AOX by Phenothiazines

The percent of inhibition of a group of phenothiazines consisting of chlorpromazine, perphenazine, promethazine, thioridazine, and trifluoperazine on rat liver AOX and XO has been evaluated and the results are set out in Table 1. The maximum initial velocity for the oxidation of benzaldehyde and phenanthridine by AOX were found to be 14.4 ± 2.3 and 39.2 ± 3.7 nM/min/mg protein, respectively. All the tested compounds could inhibit AOX activity measured either by phenanthridine or benzaldehyde as the substrates with almost no effects on XO activity. Interestingly, in the case of all the phenothiazines, more inhibition was observed with the benzaldehyde as an aldehyde substrate compared with phenanthridine, the N-heterocycle substrate. These results were contrary to that obtained with menadione as one of the common inhibitors of AOX, whose inhibition was higher with the N-heterocyclic substrate. Using phenanthridine as the substrate, the highest and lowest inhibitions were observed with perphenazine and trifluoperazine, respectively. The corresponding values with the benzaldehyde oxidation were obtained with promethazine and trifluoperazine, respectively. No inhibition was observed in the XO activity in the presence of either of the phenothiazines.

The oxidation rate of xanthine increased by 31% in the presence of menadione. This enhancing effect of menadione was almost completely inhibited in the presence of 100 µM allopurinol. It has been shown that menadione acts as an electron acceptor of XO and increases the rate of xanthine oxidation [38].

The inhibition patterns were well reflected in the IC_{50} values (Table 2). In the case of benzaldehyde oxidation, the smallest and largest IC_{50} values were exhibited by promethazine and trifluoperazine, respectively; whereas perphenazine and trifluoperazine produced the lowest and highest IC_{50} values, respectively, against AOX-catalyzed phenanthridine oxidation.

The ratio of IC_{50} values for phenanthridine and benzaldehyde oxidations was also calculated to determine the relative ability of the tested phenothiazines to discriminate between their inhibitory effects on the N-heterocycle and aldehyde oxidations. Larger values of the IC_{50} ratio represent more discrimination between the inhibitory effects of the phenothiazine on phenanthridine and benzaldehyde oxidation catalyzed by AOX. Interestingly, large values were obtained for the IC_{50} ratios with almost all the phenothiazines. Apart from perphenazine, all the other IC_{50} ratios fell into the range of 8–14. The ratio of IC_{50} values of phenanthridine to benzaldehyde oxidations for perphenazine was calculated as 3. This means that all the tested phenothiazines could inhibit benzaldehyde oxidation more potently than phenanthridine oxidation.

In order to further investigate the inhibitory characteristics of phenothiazines on the benzaldehyde oxidation by rat liver AOX, the enzymatic kinetic parameters were also determined spectrophotometrically from a Lineweaver–Burk double reciprocal plot of 1/V against 1/[S] (Table 3).

AOX was inhibited by the tested phenothiazines in different manners. Both chlorpromazine and trifluoperazine exerted their inhibitory effects on the AOX-catalyzed oxidation of benzaldehyde in a non-competitive inhibitory manner with kinetic constants of 0.79 and 6.5 µM, respectively.

However, the oxidation was inhibited by promethazine and thioridazine in a mixed manner (competitive–noncompetitive type) with kinetic constants of $K_i < K_I$. Perphenazine was found to be an uncompetitive inhibitor of the benzaldehyde oxidation with a K_i value of 0.29 µM. AOX has a relatively large active/binding site with a marked flexibility and distinct binding sites for both its substrates and inhibitors. A variation in the active site of AOX isoforms has also been postulated [39]. These may account for the various types of inhibition observed for the tested phenothiazines towards AOX activity.

Table 2 The half-maximal inhibitory concentration (IC_{50}) values for inhibition of rat liver aldehyde oxidase-catalyzed oxidations of phenanthridine and benzaldehyde with some phenothiazines

Name	IC_{50} (µM)		Ratio[a]
	Phenanthridine oxidation	Benzaldehyde oxidation	
Chlorpromazine	11.4	1.0	11
Perphenazine	4.3	1.4	3
Promethazine	8.2	0.9	9
Thioridazine	15.1	1.8	8
Trifluoperazine	49.6	3.6	14

[a]Ratio of IC_{50} for phenanthridine oxidation and IC_{50} for benzaldehyde oxidation

Table 3 Inhibition kinetic parameters of the inhibitory activity of phenothiazines on the oxidation of benzaldehyde by rat liver aldehyde oxidase (AOX) for the AOX inhibition

Name	Inhibition type	K_i (µM)	K_I (µM)
Chlorpromazine	Non-competitive	0.79	0.79
Perphenazine	Uncompetitive	0.29	–
Promethazine	Mixed	1.91	2.9
Thioridazine	Mixed	1.41	5.2
Trifluoperazine	Non-competitive	6.5	6.5

K_i dissociation constant of the enzyme–inhibitor complex, K_I dissociation constant of the enzyme–substrate–inhibitor complex
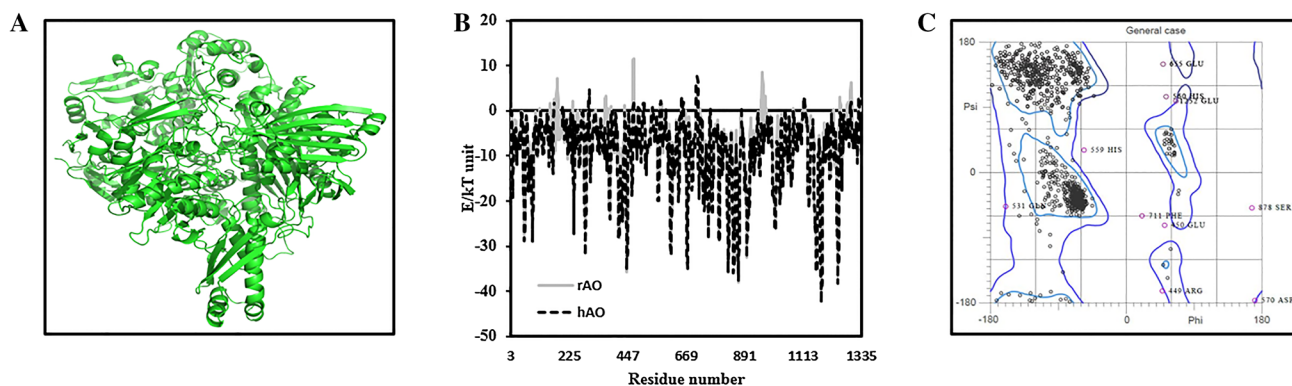
Fig. 2 a Cartoon representation of modeled rat AOX1 based on homology modeling using human AOX1 (PDB ID: 4UHX). b ANOLEA energy profile of rat AOX1 model. c Ramachandran plot of modeled rat AOX obtained from the MolProbity model evaluation server. The results show that 98.9% of amino acids are in the allowed regions. *AOX* aldehyde oxidase

Table 4 The outlier residues on rat aldehyde oxidase 1 (AOX1) based on the predicted model human AO X1 crystal structure, 4UHX, in the Ramachandran plot

Human AOX1 crystal structure 4UHX			Rat AOX1 predicted model		
Residue	Phi	Psi	Residue	Phi	Psi
Glu^{451}*	49.2	− 65.8	Ser^{197}	− 149.6	− 35.3
Gln^{532}*	− 162.8	− 50.8	Pro^{198}	− 0.1	94.2
Val^{811}*	− 131.9	− 86.8	Gln^{228}	− 64.8	91.2
Arg^{921}	− 37.6	105.3	Arg^{449}	48.9	− 164.9
Gln^{1257}*	62.3	101.5	Glu^{450}*	51.4	− 73.2
			Gln^{531}*	− 160.1	− 47.3
			His^{559}	− 56.3	31.5
			His^{560}	53.1	105.4
			Asp^{570}	171.4	− 177.5
			Glu^{655}	49.9	150.5
			Phe^{711}	21.8	− 60.2
			Val^{806}*	− 131.1	− 86.7
			Ser^{878}	167.2	− 49.9
			Glu^{1252}*	66.7	99.2

*The residues which were outliers in both structures

3.2 Evaluation of Predicted 3D Structure of Rat AOX1 by Homology Modeling

In order to understand the interaction modes between the phenothiazines and rat AOX1, a homology-based model of the enzyme was built using human AOX as the template [27], and a cartoon representation of the proposed model is illustrated in Fig. 2. The quality of the model structure of rat AOX1 and the crystallographic structure of human AOX (as template) was assessed by means of different metrics, such as a Ramachandran diagram and ANOLEA energy profile (Fig. 2). According to the Ramachandran plot for the predicted rat AOX1 model, 94.2 and 98.9% of all residues are in favored and allowed regions, respectively, while in the case of human AOX crystal structure, these values are 96.8 and 99.6%. Fourteen residues in the rat AOX model structure are outliers in terms of phi and psi angles, while there are only five outliers in the human AOX crystallography structure (Table 4). None of the outlier residues in the model structure are involved in ligand interaction, and four of them are in common with the human AOX experimental structure (see Table 1; Fig. 2).

Comparing the ANOLEA energy profile of the rat AOX1 model to that of the human AOX structure indicates an acceptable score for almost all the rat AOX1 model residues with the exception of the residues for which there was no equivalent residue in the template structure. Furthermore, all the rat AOX1 model outlier residues were located out of the ligand binding site (Fig. 2).

3.3 Molecular Docking

The results of docking experiments performed by the GOLD program showed that Leu^{574}, Gln^{576}, Asp^{577}, Ser^{1055}, Arg^{1056}, Lys^{1059}, Met^{1060}, and Pro^{1061} residues of rat aldehyde oxidase are involved in hydrophobic interactions with all the examined phenothizaines. Moreover, in all the phenothizaines except chlorpromazine, Trp^{1120} also participates in a hydrophobic interaction. Other hydrophobic interactions are Gly^{1115} with perphenazine and trifluroprazine and Thr^{1116} with perphenazine. Among all the phenothiazines, the only hydrogen bond was observed in perphenazine with Trp^{1117}. This residue is also involved in hydrophobic interactions with thioridazine and trifluropraizne. The outlined interactions observed in the docking studies are presented in Fig. 3.
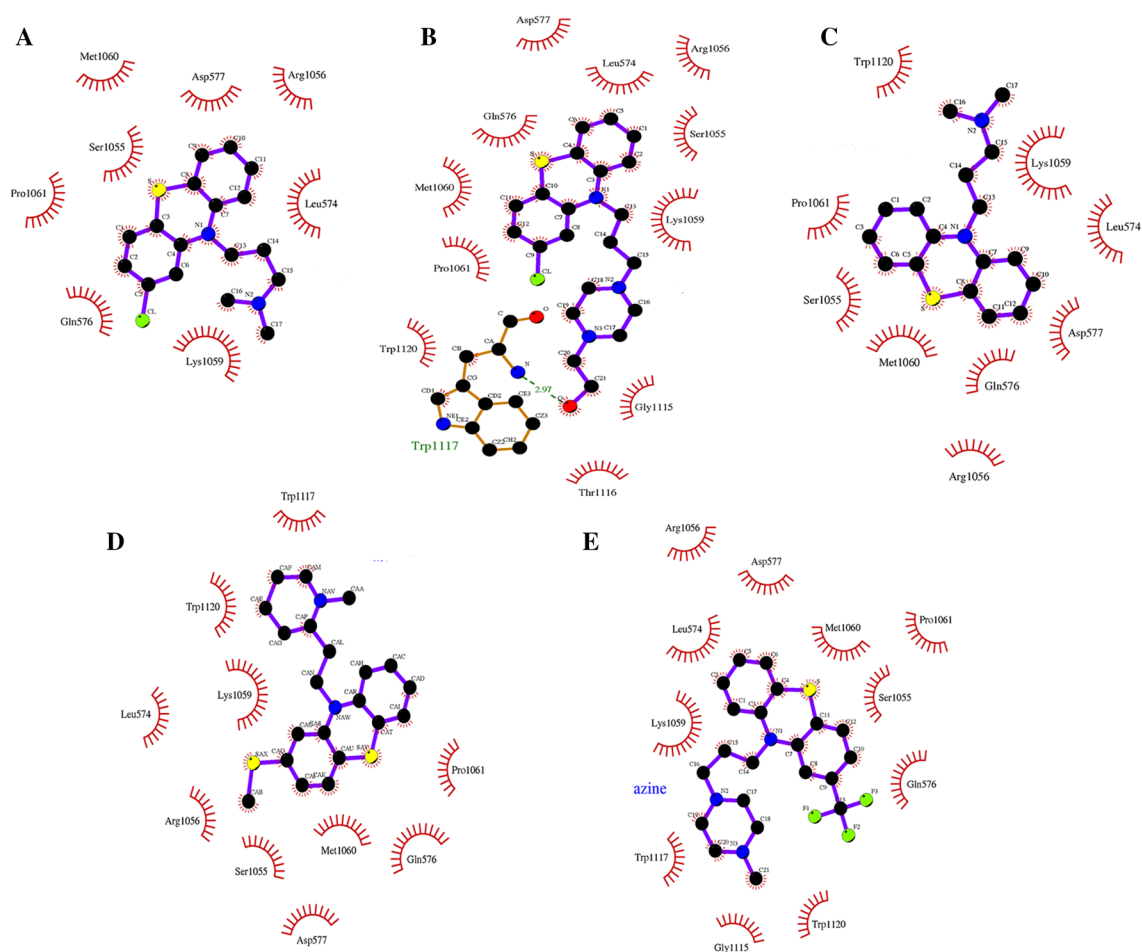
Fig. 3 A 2D illustration of the interactions between chlorpromazine (**a**), perphenazine (**b**), promethazine (**c**), thioridazine (**d**) and trifluoperazine (**e**) in the binding site of rat aldehyde oxidase

4 Discussion

Due to some changes in medicinal chemistry strategies, the role of non-CYP enzymes has become more remarkable. AOX is one of these enzymes that has recently received great attention in drug discovery programs due to the increasing number of compounds metabolized by this enzyme, along with renewed interest in the physiological function of AOX [12]. Accordingly, finding the inhibition profile of those compounds that interfere with AOX activity would be of great value.

On the other hand, substrate-dependent inhibition profiles in drug-metabolizing enzymes and in vitro drug–drug interaction predictions are generally a known phenomenon. AOX activity is highly substrate-dependent and the enzyme activity from various species towards different substrates shows a wide range of activity. Therefore, the selection of an appropriate substrate for AOX-based drug–drug interaction studies is a critical issue. However, these important aspects of AOX have not received enough attention. Therefore, in

the present study, the interaction of some phenothiazines with AOX has been investigated. As the substrates of AOX fall into two major groups of aldehydes and N-heterocyclic compounds, this study has covered the interaction of pheno-thiazines with both benzaldehyde (as an aldehyde substrate) and phenanthridine (as an N-heterocyclic substrate).

All six investigated phenothiazines could inhibit AOX activity towards both substrates. None of the tested pheno-thiazines could inhibit XO. However, Coelho et al. [27] have shown the inhibitory effect of thioridazine on pure bovine XO, although the inhibition was about 10- to 20-fold weaker than the human aldehyde oxidase-catalyzed oxidation of phthalazine. Interestingly, all the phenothiazines inhibited benzaldehyde oxidation more strongly than phenanthridine oxidation. These results were in contrast to those obtained with menadione, a putative inhibitor of AOX. This differ-ence in the inhibitory effects of the phenothiazines on AOX-mediated oxidations of phenanthridine and benzaldehyde may arise from different interaction modes of the drugs with the binding sites of the enzyme. It may also result from the

oxidation of phenanthridine and benzaldehyde by different isoforms of AOX, each with its own binding characteristics. The rat has been employed in AOX-catalyzed metabolism studies during the development of potential drugs; however, in some cases, this animal does not serve as an appropriate animal model for human AOX. Rat AOX also differs from that of human in terms of its isoforms. Like rabbit, two isoforms have been reported for rat, AOX1 and AOX3, whereas humans possess a single enzyme (AOX1).

Although partially purified AOX was used in this study, the enzyme activity towards both substrates can be attributed to AOX. Aldehyde dehydrogenase is also able to oxidize aldehydes, but its activity towards aromatic aldehydes like benzaldehyde is low and, more importantly, it needs $NADH/NAD^+$ as its cofactor. In addition, for the preparation of AOX in this study, the enzyme fraction was heated at 55–57 °C for 10 min; however, aldehyde dehydrogenase is not a thermostable enzyme and it is no longer able to perform the desired tasks after exposure to heat stress. Cytochrome P450 can metabolize phenanthridine to several metabolites, but the enzyme uses $NADPH/NADP^+$ as its cofactor; furthermore, the enzyme is thermosensitive and denatures easily into its inactive form. Therefore, under the conditions used in the present study, the oxidations of benzaldehyde and phenanthridine occur with AOX.

Few studies [40, 41] have investigated the differences in the effects of AOX inhibitors on the AOX-catalyzed oxidation of aldehydes and N-heterocycles as the two major groups of enzyme substrates. In these studies, the inhibitory effects of some flavonoids were studied using vanillin (another aldehyde substrate of AOX) and phenanthridine as the AOX substrates. Based on these studies, the vanillin oxidation was inhibited more strongly than phenanthridine by the tested flavonoids. Hamzeh-Mivehroud et al. [40] attributed this substrate-dependent difference in the inhibitory effects to the binding mode of the two substrates. According to these authors, hydrophobic interactions are the most important intermolecular forces involved in the binding of phenanthridine to the AOX active site, while vanillin binds mostly through hydrogen bonds to the enzyme.

The inhibitory effects of phenothiazines on AOX activity have been reported by others. Johns showed that 5 μM chlorpromazine can inhibit both benzaldehyde and N-methylphenazine oxidations catalyzed by human and rabbit liver AOX at about 50% [21]. Trifluoperazine caused more inhibition on benzaldehyde oxidation than N-methylphenazine oxidation (72 vs. 30%) by human liver AOX; however, the inhibition of the rabbit liver was found to be 63 and 70% for benzaldehyde and N-methylphenazine oxidations, respectively. With promethazine, the N-heterocyclic substrate oxidation was inhibited slightly more potently than the aldehyde substrate metabolism by both human and rabbit liver AOX [21]. These results indicate that the inhibitory effects of the studied phenothiazines on AOX activity are substrate- and species-dependent, and it is difficult to interpret these types of findings with a single model.

In a study carried out by Obach et al. [20], the inhibitory effects of 239 compounds including some phenothiazines on human liver AOX were studied. The IC_{50} values reported in this study for the phenothiazines were lower than our results. The differences in the results may have originated from the differences in the substrates and enzyme sources used in two studies.

To evaluate potential drug interactions using in vitro assessment of the inhibition of AOX by the tested phenothiazines, the ratio of the concentration of the inhibitors in vivo, [I], to the inhibition constant, K_i, (obtained for phenanthridine oxidation) was used [13]. The inhibitor concentrations used were as follows: (chlorpromazine) = 0.5 μM [42], (perphenazine) = 20 nM [43], (promethazine) = 81 nM [44], (thioridazine) = 1.7 nM [45], and (trifluoperazine) = 7 nM [46]. For all tested drugs, apart from chlorpromazine, the $[I]/K_i$ values obtained were around 1. This ratio for chlorpromazine was calculated as 0.63. A value of ≥ 1 is considered high risk for drug interactions, and a value of 0.1–1 is considered moderate risk. If this value falls to less than 0.1, a low risk of drug interactions is expected, generally indicating that there is no need for further in vivo study [13], as there is less likely to have a drug–drug interaction if these phenothiazines are co-administered with those drugs that were metabolized by AOX. However, the highest concentration of AOX is found in liver, and the concentration of drugs in liver, as the major metabolic site for most drugs during the absorptive phase, may easily reach a higher level than its concentration in the blood [13]. Therefore, the potential of drug–drug interaction for chlorpromazine cannot be ruled out, and further study is required to judge the implications of these results to clinical drug interactions.

To determine the mode of interactions between phenothiazines and rat AOX, a combination of homology modeling and molecular docking was performed. In one study carried out by Coelho et al. in [27], they indicated that the binding site of thioridazine is near the dimer interference in a groove, which is located at the enzyme surface, between two loops (formed by residues 570–580 and 1058–1067), and that it is far from the active site. They also showed that, upon inhibitor binding, the binding pocket will be more accessible by movement of the side chains from the His^{575} and Glu^{577} residues. Also, the presence of some residues in the 570 and 571 positions helps in the formation of helical turns close to the thioridazine inhibitor binding site, upon thioridazine binding, and, furthermore, Pro^{576} for conferring extra flexibility to the loop containing 570–580 residues is of great importance. They proposed a similar mode of inhibition and the same binding site for other drugs with tricyclic ring-based scaffolds similar to thioridazine [27].

To predict the interactions between phenothiazines and rat AOX, homology modeling was performed to obtain the 3D structure of rat AOX. Our proposed model showed favorable properties from geometrical point of view which was used for docking studies. The involved residue in the interaction were Leu^{574}, Gln^{576}, Asp^{577}, Ser^{1055}, Arg^{1056}, Lys^{1059}, Met^{1060}, and Pro^{1061} for phenothiazine, Glu^{1115} for perphenazine and trifuroprazine, Thr^{116} for perphenaizne, Trp^{1117} for thioridazine, perphenazine and trifulroprazine, and Trp^{1120} for all the drugs except chlorpromazine. All the interactions (except the Trp^{1117} interaction with perphenizne) were hydrophobic which demonstrates the importance of such interactions in the inhibition of AOX.

It was shown that the protein–protein association site is a dimerization site and, in the case of mouse AOX1 residues located in the dimerization site ($mAOX1 Arg^{1068}$, Gly^{1069} and Glu^{1073}), are important for the association of the two monomers in forming the homodimer, and it has generally been accepted that residue interment in the protein interface between two monomers with exposed areas above 40 Å are important in the dimerization process [13, 14]. As in this work, the binding site of phenothiazines is near the dimer interference, it is likely that the residues buried in this site are major contributors to the dimerization process. It is generally accepted that all the catalytically active form of AOX is a homodimer [47, 48], although the reason why AOXs are homodimers is unknown, as it has been proven that the monomeric subunit is functionally active [49], and therefore the studied drugs in this work may inhibit the dimerization process and prevent AOX action.

5 Conclusion

In summary, five important phenothiazine drugs (i.e., trifluperazine, chlorpromazine, perphenazine, thioridazine, and promethazine) can inhibit AOX activity measured either by benzaldehyde, an aldehyde compound, or by phenanthridine, an N-heterocycle, as the substrates. With all the tested phenothiazines (except perphenazine), the ratio of the IC_{50} value for phenanthridine to that for benzaldehyde was found to be around 10, while the value for perphenazine was 3. This indicates that phenothiazines have dual inhibitory effects on AOX activity towards aldehydes and N-heterocycles as the two major classes of enzyme substrates. Although AOX and XO have many common properties, no inhibition was observed on XO activity with any of the five phenothiazines. The mode of interactions for phenothiazine-related drugs and AOX in the binding pocket was identified and the results showed that most of interactions are of a hydrophobic nature.

References

1. Argikar UA, Potter PM, Hutzler JM, Marathe PH. Challenges and opportunities with non-CYP enzymes aldehyde oxidase, carboxylesterase, and udp-glucuronosyltransferase: focus on reaction phenotyping and prediction of human clearance. AAPS J. 2016;18(6):1391–405. https://doi.org/10.1208/s12248-016-9962-6.

2. Cerny MA. Prevalence of non-cytochrome P450-mediated metabolism in food and drug administration-approved oral and intravenous drugs: 2006–2015. Drug Metab Dispos. 2016;44(8):1246–52. https://doi.org/10.1124/dmd.116.070763.

3. Gan J, Ma S, Zhang D. Non-cytochrome P450-mediated bioactivation and its toxicological relevance. Drug Metab Rev. 2016;48(4):473–501. https://doi.org/10.1080/03602532.2016.1225756.

4. Taylor AP, Robinson RP, Fobian YM, Blakemore DC, Jones LH, Fadeyi O. Modern advances in heterocyclic chemistry in drug discovery. Org Biomol Chem. 2016;14(28):6611–37. https://doi.org/10.1039/c6ob00936k.

5. Rashidi MR, Smith JA, Clarke SE, Beedham C. In vitro oxidation of famciclovir and 6-deoxypenciclovir by aldehyde oxidase from human, guinea pig, rabbit, and rat liver. Drug Metab Dispos. 1997;25(7):805–13.

6. Beedham C, Miceli JJ, Obach RS. Ziprasidone metabolism, aldehyde oxidase, and clinical implications. J Clin Psychopharmacol. 2003;23(3):229–32. https://doi.org/10.1097/01.jcp.0000084028.22282.f2.

7. Rashidi MR, Beedham C, Smith JS, Davaran S. In vitro study of 6-mercaptopurine oxidation catalysed by aldehyde oxidase and xanthine oxidase. Drug Metab Pharmacokinet. 2007;22(4):299–306.

8. Klecker RW, Cysyk RL, Collins JM. Zebularine metabolism by aldehyde oxidase in hepatic cytosol from humans, monkeys, dogs, rats, and mice: influence of sex and inhibitors. Bioorg Med Chem. 2006;14(1):62–6. https://doi.org/10.1016/j.bmc.2005.07.053.

9. Jordan CG, Rashidi MR, Laljee H, Clarke SE, Brown JE, Beedham C. Aldehyde oxidase-catalysed oxidation of methotrexate in the liver of guinea-pig, rabbit and man. J Pharm Pharmacol. 1999;51(4):411–8.

10. Garattini E, Terao M. Increasing recognition of the importance of aldehyde oxidase in drug development and discovery. Drug Metab Rev. 2011;43(3):374–86. https://doi.org/10.3109/03602532.2011.560606.

11. Garattini E, Terao M. The role of aldehyde oxidase in drug metabolism. Expert Opin Drug Metab Toxicol. 2012;8(4):487–503. https://doi.org/10.1517/17425255.2012.663352.

12. Rashidi MR, Soltani S. An overview of aldehyde oxidase: an enzyme of emerging importance in novel drug discovery. Expert Opin Drug Discov. 2017;12(3):305–16. https://doi.org/10.1080/17460441.2017.1284198.

13. Barr JT, Jones JP. Inhibition of human liver aldehyde oxidase: implications for potential drug–drug interactions. Drug Metab Dispos. 2011;39(12):2381–6. https://doi.org/10.1124/dmd.111.041806.

14. Glintborg B, Andersen SE, Dalhoff K. Drug–drug interactions among recently hospitalised patients–frequent but mostly clinically insignificant. Eur J Clin Pharmacol. 2005;61(9):675–81. https://doi.org/10.1007/s00228-005-0978-6.

15. McCance-Katz EF, Sullivan LE, Nallani S. Drug interactions of clinical importance among the opioids, methadone and buprenorphine, and other frequently prescribed medications: a review. Am J Addict. 2010;19(1):4–16. https://doi.org/10.1111/j.1521-0391.2009.00005.x.

16. Cascorbi I. Drug interactions–principles, examples and clinical consequences. Dtsch Arzteblatt Int. 2012;109(33–34):546–55. https://doi.org/10.3238/arztebl.2012.0546 (quiz 56).

17. Siah M, Farzaei MH, Ashrafi-Kooshk MR, Adibi H, Arab SS, Rashidi MR, et al. Inhibition of guinea pig aldehyde oxidase activity by different flavonoid compounds: an in vitro study. Bioorg Chem. 2016;64:74–84. https://doi.org/10.1016/j.bioorg.2015.12.004.

18. Tayama Y, Sugihara K, Sanoh S, Miyake K, Morita S, Kitamura S, et al. Effect of tea beverages on aldehyde oxidase activity. Drug Metab Pharmacokinet. 2011;26(1):94–101.

19. Nirogi R, Kandikere V, Palacharla RC, Bhyrapuneni G, Kanamarlapudi VB, Ponnamaneni RK, et al. Identification of a suitable and selective inhibitor towards aldehyde oxidase catalyzed reactions. Xenobiotica. 2014;44(3):197–204. https://doi.org/10.3109/00498254.2013.819594.

20. Obach RS, Huynh P, Allen MC, Beedham C. Human liver aldehyde oxidase: inhibition by 239 drugs. J Clin Pharmacol. 2004;44(1):7–19. https://doi.org/10.1177/0091270003260336.

21. Johns DG. Human liver aldehyde oxidase: differential inhibition of oxidation of charged and uncharged substrates. J Clin Invest. 1967;46(9):1492–505. https://doi.org/10.1172/jci105641.

22. Barr JT, Jones JP. Evidence for substrate-dependent inhibition profiles for human liver aldehyde oxidase. Drug Metab Dispos. 2013;41(1):24–9. https://doi.org/10.1124/dmd.112.048546.

23. Pirouzpanah S, Rashidi MR, Delazar A, Razavieh SV, Hamidi A. Inhibitory effects of *Ruta graveolens* L. extract on guinea pig liver aldehyde oxidase. Chem Pharm Bull. 2006;54(1):9–13.

24. Johnson C, Stubley-Beedham C, Stell JG. Hydralazine: a potent inhibitor of aldehyde oxidase activity in vitro and in vivo. Biochem Pharmacol. 1985;34(24):4251–6.

25. Altschul SF, Gish W, Miller W, Myers EW, Lipman DJ. Basic local alignment search tool. J Mol Biol. 1990;215(3):403–10. https://doi.org/10.1016/s0022-2836(05)80360-2.

26. Wu CH, Apweiler R, Bairoch A, Natale DA, Barker WC, Boeckmann B, et al. The Universal Protein Resource (UniProt): an expanding universe of protein information. Nucleic Acids Res. 2006;34((Database issue)):D187–91. https://doi.org/10.1093/nar/gkj161.

27. Coelho C, Foti A, Hartmann T, Santos-Silva T, Leimkuhler S, Romao MJ. Structural insights into xenobiotic and inhibitor binding to human aldehyde oxidase. Nat Chem Biol. 2015;11(10):779–83. https://doi.org/10.1038/nchembio.1895.

28. Sievers F, Wilm A, Dineen D, Gibson TJ, Karplus K, Li W, et al. Fast, scalable generation of high-quality protein multiple sequence alignments using Clustal Omega. Mol Syst Biol. 2011;7:539. https://doi.org/10.1038/msb.2011.75.

29. Schwede T, Kopp J, Guex N, Peitsch MC. SWISS-MODEL: an automated protein homology-modeling server. Nucleic Acids Res. 2003;31(13):3381–5.

30. Davis IW, Leaver-Fay A, Chen VB, Block JN, Kapral GJ, Wang X, et al. MolProbity: all-atom contacts and structure validation for proteins and nucleic acids. Nucleic Acids Res. 2007;35((Web Server issue)):W375–83. https://doi.org/10.1093/nar/gkm216.

31. Melo F, Devos D, Depiereux E, Feytmans E. ANOLEA: a www server to assess protein structures. Proc Int Conf Intell Syst Mol Biol. 1997;5:187–90.

32. Froimowitz M. HyperChem: a software package for computational chemistry and molecular modeling. Biotechniques. 1993;14(6):1010–3.

33. Allinger NL. Conformational analysis. 130. MM2. A hydrocarbon force field utilizing V1 and V2 torsional terms. J Am Chem Soc. 1977;99(25):8127–34. https://doi.org/10.1021/ja00467a001.

34. Dewar MJS, Thiel W. Ground states of molecules. 39. MNDO results for molecules containing hydrogen, carbon, nitrogen, and oxygen. J Am Chem Soc. 1977;99(15):4907–17. https://doi.org/10.1021/ja00457a005.

35. O'Boyle NM, Banck M, James CA, Morley C, Vandermeersch T, Hutchison GR. Open Babel: an open chemical toolbox. J Cheminform. 2011;3:33. https://doi.org/10.1186/1758-2946-3-33.

36. Grant JA, Gallardo MA, Pickup BT. A fast method of molecular shape comparison: a simple application of a Gaussian description of molecular shape. J Comput Chem. 1996;17(14):1653–66. https://doi.org/10.1002/(sici)1096-987x(19961115)17:14%3c1653:aid-jcc7%3e3.0.co;2-k.

37. Wallace AC, Laskowski RA, Thornton JM. LIGPLOT: a program to generate schematic diagrams of protein–ligand interactions. Protein Eng. 1995;8(2):127–34.

38. Si Yoshihara, Tatsumi K. Kinetic and inhibition studies on reduction of diphenyl sulfoxide by guinea pig liver aldehyde oxidase. Arch Biochem Biophys. 1986;249(1):8–14. https://doi.org/10.1016/0003-9861(86)90554-0.

39. Garattini E, Mendel R, Romao MJ, Wright R, Terao M. Mammalian molybdo-flavoenzymes, an expanding family of proteins: structure, genetics, regulation, function and pathophysiology. Biochem J. 2003;372(Pt 1):15–32. https://doi.org/10.1042/bj20030121.

40. Hamzeh-Mivehroud M, Rahmani S, Feizi MA, Dastmalchi S, Rashidi MR. In vitro and in silico studies to explore structural features of flavonoids for aldehyde oxidase inhibition. Arch Pharm. 2014;347(10):738–47. https://doi.org/10.1002/ardp.201400076.

41. Pirouzpanah S, Hanaee J, Razavieh SV, Rashidi MR. Inhibitory effects of flavonoids on aldehyde oxidase activity. J Enzyme Inhib Med Chem. 2009;24(1):14–21. https://doi.org/10.1080/14756360701841301.

42. Brunton LL, Gilman A, Goodman LS. Goodman and Gilman's the pharmacological basis of therapeutics. New York: McGraw-Hill; 2006.

43. Eggert Hansen C, Rosted Christensen T, Elley J, Bolvig Hansen L, Kragh-Sorensen P, Larsen NE, et al. Clinical pharmacokinetic studies of perphenazine. Br J Clin Pharmacol. 1976;3(5):915–23.

44. Wallace JE, Shimek EL Jr, Harris SC, Stavchansky S. Determination of promethazine in serum by liquid chromatography. Clin Chem. 1981;27(2):253–5.

45. Daniel WA, Syrek M, Haduch A, Wojcikowski J. Pharmacokinetics and metabolism of thioridazine during co-administration of tricyclic antidepressants. Br J Pharmacol. 2000;131(2):287–95. https://doi.org/10.1038/sj.bjp.0703540.

46. Midha KK, Korchinski ED, Verbeeck RK, Roscoe RM, Hawes EM, Cooper JK, et al. Kinetics of oral trifluoperazine disposition in man. Br J Clin Pharmacol. 1983;15(3):380–2.

47. Cerqueira NM, Coelho C, Bras NF, Fernandes PA, Garattini E, Terao M, et al. Insights into the structural determinants of

substrate specificity and activity in mouse aldehyde oxidases. J Biol Inorg Chem. 2015;20(2):209–17. https://doi.org/10.1007/s00775-014-1198-2.

48. Kurosaki M, Bolis M, Fratelli M, Barzago MM, Pattini L, Perretta G, et al. Structure and evolution of vertebrate aldehyde oxidases: from gene duplication to gene suppression. Cell Mol Life Sci. 2013;70(10):1807–30. https://doi.org/10.1007/s0001 8-012-1229-5.

49. Garattini E, Fratelli M, Terao M. Mammalian aldehyde oxidases: genetics, evolution and biochemistry. Cell Mol Life Sci. 2008;65(7–8):1019–48. https://doi.org/10.1007/s0001 8-007-7398-y.